Supporting Information

Fluorine confined catalytic sites for augmented p-d hybridization promoting flow-type aqueous Zn-CO_2 batteries

Sidra Hameed,[a] Di Li,[a] Muhammad Kashif Aslam,[b] Sheng Chen,[a] Jingjing Duan[a,*]

[a] School of Energy and Power Engineering, MIIT Key Laboratory of Thermal Control of Electronic Equipment, Nanjing University of Science and Technology, Nanjing 210094, P. R. China.

[b]Department of Chemical and Petroleum Engineering, College of Engineering, UAE University, Al Ain 15551, Abu Dhabi, United Arab Emirates.

Corresponding Author e-mail address: jingjing.duan@njust.edu.cn

Figure captions

Figure S1. SEM images and EDX mapping of Zn, F, O and C of Zn-TFBDC.

Figure S2. SEM image and its EDS mapping of Zn, O and C of Zn-BDC.

Figure S3. High resolution XPS spectra of Zn-TFBDC. (a) XPS survey spectrum; (b) O 1s spectrum.

Figure S4. High resolution XPS spectra of Zn-BDC. (a) XPS survey spectrum; (b) Zn 2p; (c) C 1s; and (d) O 1s spectrum.

Figure S5. LSV curves of eCO_2RR using the Zn-TFBDC and Zn-BDC catalysts under CO_2 supply.

Figure S6. FE% of Zn-BDC promoted eCO_2RR at a potential window of -1 to -2.75 V vs RHE.

Figure S7. (a) The FE_{CO} and (b) FE_{H2} of eCO_2RR catalyzed by Zn-BDC and Zn-TFBDC.

Figure S8. NMR spectra of eCO_2RR products using (a) Zn BDC, and (b) Zn-TFBDC catalysts under CO_2 supply.

Figure S9. Modelling configurations for (a) Zn-BDC and (b) Zn-TFBDC.

Figure S10. Density of state (DOS) profile for Zn-BDC.

Figure S11. The pH value measured at different time during CO_2 dissolution.

Figure S12. (a) OCP curves of the Zn-BDC constructed AZCB against CO_2 and Ar gases; (b) Discharge response along power density.

Figure S13. Polarization charge and discharge curves for AZCBs using Zn-BDC and Zn-TFBDC.

Figure S14. Power density curves for AZCBs using Zn-BDC and Zn-TFBDC.

Figure S15. Overall charge and discharge response at different current densities for the AZCB using Zn-TFBDC.

Figure S16. Galvanostatic discharge-charge cyclability curve at a current density of 0.5 mA cm^{-2} for Zn-BDC constructed AZCB.

Figure S17. Comparison of power densities between this work and reported data with CO as the eCO_2RR product.

Figure S18. Digital photograph for single bulb illuminated by three series of An-TFBDC AZCBs.

Table S1. Comparison of FE_{HCOO-} of eCO_2RR using as-prepared catalysts.

Table S2. Performance summary of reported AZCB.

Experimental Section

Chemicals

Zinc nitrate hexahydrate $Zn(NO_3)_2.6H_2O$, 2,3,5,6-tetrafluoroterephathalic acid (TFBDC, 97%), 2,4-dihydroxyterephathalic acid (BDC), absolute ethanol (C_2H_5OH) were purchased from SCR, Chemical (ptv) Ltd, acetonitrile (CH_3CN) (chromatographic grade ≥ 99.9%), potassium bicarbonate ($KHCO_3$), and isopropanol were purchase from Aladdin chemical Co, Ltd. Nafion and de-ionized water, carbon dioxide (CO_2 99.999%) purity were used. All chemicals are analytical grade and used without any further purification.

Synthesis of catalytic materials

Zn-TFBDC: Zn-TFBDC was synthesized using hydrothermal method. Typically, 1.205 g of $Zn(NO_3)_2.6H_2O$ and 0.36g of tetrafluoroterephthalic acid (TFBDC) were dissolved in 80ml of a solvent mixture, containing absolute ethanol (C_2H_5OH), Acetonitrile (CH_3CN) and de-ionized water in a ratio of (1:1:1) under sonication until a clear solution was obtained. Then, solution was transferred to 100ml of Teflon enclosed in a stainless-steel autoclave and keep at 120°C for 12h (**Figure 1a**). After cold down at room temperature the MOF was collected using centrifuge method and washed with distilled water and ethanol for several time and dried under vacuum at 60°C for 24h.

Zn-BDC: Zn-BDC was also synthesized using the same method as Zn-TFBDC synthesis.

Preparation for working electrodes

A homogenous ink of catalytic material was prepared by dispersing 10mg catalyst in a mixture of isopropanol and distilled water mixture (3:1 ratio), followed by addition of 40μL Nafion. The solution was ultrasonicated for 2 h. A 400 μL homogenous catalyst ink was finely sprayed onto a 1cm x 1cm carbon paper with a PTFE layer.

Characterization

X-ray diffraction (XRD) was carried out using a Philips 1130 diffractometer at 40kV, 25mA (λ= 1.5418A) with Cu-Kα radiations (XRD, BRUKER AXS company). The Morphology of the synthesized MOF was analyzed using a field emission scanning electron microscope (FESEM, JEOL 6380). Fournier transform infrared (FTIR) spectroscopy was performed using an FTIR, Nicolet 6700, spectrometer. X-ray photoelectron spectroscopy (XPS, Thermo Kalpha; Thermo ESCALAB 250XI; Axis Ultra DLD Kratos AXIS SUPRA; PHI-5000versaprobeIII) was conducted to confirm the oxidation state of the atoms.

The eCO_2RR measurements

Electrochemical measurements of the electrocatalyst were conducted using a CHI electrochemical workstation (CH760e) with a three-chamber electrolytic flow cell. Nikel foam and Ag/AgCl electrode were used as the counter electrode and reference electrode, respectively. The working and counter electrodes were separated by a Nafion 117 membrane. A 20ml aqueous solution of 0.5 M $KHCO_3$ was used as the electrolyte in each half cell. During the electrochemical reduction testing, CO_2 was supplied at a flow rate of 80sscm, while the electrolyte flow rate was maintained 5mL min^{-1}. Linear sweep voltammetry (LSV) was recorded over a potential range of 0 to -3V at a scan rate of 5 m Vs^{-1}. Electrochemical impedance (EIS) measurement was conducted over a frequency range of 0.01Hz to 10^6 Hz at an applied potential of -1V. All potentials for CO_2 reduction in this study were converted to the reversible hydrogen electrode (RHE) potential using the following equation.

$$E_{RHE} = E_{Ag/AgCl} + 0.0591 \times PH + 0.197$$

in a wide range of potential from -0.75V to -2.75V.

Gas and liquid product analysis

Gas products analysis: The gaseous products were collected in airbags and analyzed using a gas chromatograph (GC, Agilent) equipped with a flame ionization detector (FID) for the quantification of CO and hydrocarbon (CH_4 & C_2 products) and a thermal conductivity detector (TCD) for the quantification of H_2. High purity Ar (99.999%) was used as the carrier gas. The Faradic efficiency (FE%) of products was calculated using the following equation.

$$FE\% = \frac{Q_{H_2,CO}}{Q_{total}} \times 100\%$$

$$=\frac{n\times N\times F}{(j\times t)}\times 100\%$$

In the above equation,

n = no. of electron transfer during eCO_2RR into H_2 and CO

N = Avogadro's number

F = Faradic constant (96485 C mol^{-1})

j = total current density

Liquid product analysis: Liquid product was analyzed using nuclear magnetic resonance (NMR) (Bruker Advance, 500M). 35µL dimethyl sulfoxide (DMSO) was used as an internal standard.

Computational Method and Model

To investigate the mechanism of the electrocatalyst in CO_2 reduction, density functional theory (DFT) calculations were performed for Zn-BDC and Zn-TFBDC using CP2K [1], A DZVP-MOLOPT basis set [2] was employed, with core electrons described by Goedecker–Teter–Hutter (GTH) pseudopotentials. [3] The plane wave cut-off and relative cutoff were set to set to 400 Ry and 50 Ry, respectively. CP2K input files were generated using Multiwfn [4], while thermodynamic corrections and zero-point energy were handled by Shermo. [5] The model structures of both electrocatalysts are shown in Figure S10, EIS. The Gibbs free energy change for each step of the eCO_2RR process is given by:

$$\Delta G=\Delta \mathrm{E}+\Delta E_{ZPE}+\Delta TS$$

The flow-type aqueous Zn-CO_2 battery (AZCB) assembly

Anode and cathode preparation:

The anode was prepared from a fresh 3×3cm zinc plate, which was mechanically polished with sand paper, then cleaned with ethanol and distilled water, and finally dried. The cathode was prepared following the same procedure as for eCO_2RR. The anolyte was the mixed solution of 6 M KOH and 0.2M Zinc acetate, while the catholyte was 0.8 M $KHCO_3$, pre-saturated with CO_2 for 3 hrs (pH = 5.4). The anode and cathode were separated by an anion exchange membrane (AEM), with each chamber filled with the respective electrolyte. Additionally, a CO_2 gas chamber was continuously supplied with CO_2 at a flow rate of 20 sccm. The charge and discharge polarizations curve was collected at 10 mV s^{-1} under continues CO_2 supply.

Theoretical energy efficiency calculation for flow type AZCB:

Theoretical energy efficiency can be calculated using the following equation:

$$EE = \frac{\Delta G_{output}}{\Delta G_{input}} = \frac{nE_{discharge}F + \Delta G_{CO_2\,splitting}}{nE_{charge}F}$$

$$\Delta G_{CO_2\,spliting} = 257.38\text{kJmol}^{-1}$$

In the real cell, competitive HER produces fuel H_2, while carbon dioxide reduction produced CO gas, considering that, battery EE can be calculated as follow:

$$EE = \frac{\Delta G_{output}}{\Delta G_{input}} = \frac{nE_{discharge}F + FE_{CO} \times \Delta G_{CO_2\,spliting} + FE_{HER} \times \Delta G_{H_2O\,spliting}}{nE_{charge}F}$$

$$\Delta G_{H_2O\,splitting} = 257.38\text{KJmol}^{-1}$$

Theoretical potential (V) calculation for flow type AZCB:

To calculate the theoretical potential (V) for the flow type AZCB, anodic and cathodic reactions are following

At the cathode (0.8 M $KHCO_3$, sat. CO_2 solution, (pH= 5.4):

Cathodic potential, during discharge at cathode for AZCB reaction will be as follow

$$CO_2 + 2H^+ + 2e^- \rightarrow CO + H_2O$$

$$E_c = E^{\theta}_{CO_2/CO} - \frac{RT}{nF}\ln\left[\frac{1}{\alpha^2_{H^+}}\right] = -0.106\text{V} - \frac{8.314\times 298.15}{2\times 96485}\ln\frac{1}{\left(10^{-5.4}\right)^2 \text{V}} = -0.425\text{V}$$

Where $E^{\theta}_{CO_2/CO} = -0.106\text{V}$ vs. SHE

At anode (6M KOH + 0.2M $(CH_3COO)_2$):

Anodic potential: during discharge at anode for Zn-CO_2 battery reaction will be as follow

$$Zn - 2e^{-} \rightarrow Zn^{2+}$$

$$Zn^{2+} + 4OH^{-} \rightarrow Zn\left(OH\right)_4^{2-}$$

$$Zn\left(OH\right)_4^{2-} \rightarrow ZnO + 2OH^{-} + H_2O$$

$$E_a = E^{\theta}_{ZnO(OH)_4^{2-}} \rightarrow \frac{RT}{nF}\ln\left[\frac{\alpha_{Zn}}{\alpha_{Zn(OH)_4^{2-}}}\right] = -1.199\text{V} - \frac{8.314\times 298.15}{2\times 96485}\ln\left[\frac{1}{0.2}\right]\text{V} = -1.219\text{V}$$

$$E^{\theta}_{ZnO(OH)_4^{2-}} = -1.199\text{V vs SHE}$$

Overall battery reaction will be as follow:

$$Zn + CO_2 + 2H^{+} + 2OH^{-} \rightarrow ZnO + CO + 2H_2O$$

The theoretical potential of battery could be:

$$E_{theo} = E_c - E_a = -0.425\text{V} - (-1.219\text{V}) = 0.794\text{V}$$

Whereas, R is 8.314JK^{-1}mol^{-1}, (molar gas constant), T = 298.15K, n =2 (total number of electrons transferred per mole of product), F = 96485 C mol^{-1} (Faradic Constant) and α is the corresponding activity.

Theoretical energy density of Zn-O_2 battery could be:

$$ED_{Zn-CO_2} = C_{Zn} \times E_{theo} = 825\text{mAh}^{-1} \times 0.794\text{V} = 655\text{Whkg}^{-1}$$

C_{Zn} is the theoretical energy density of battery based on Zn anode.

In addition, HER is also take place during battery discharging, which compete the CO2 to CO electro-conversion. At cathode HER take place as:

$$2H^{+} + 2e^{-} \rightarrow H_2$$

$$E_c = E^{\theta}_{H^{+}/H_2} - \frac{RT}{nF}\ln\left[\frac{\alpha_{H_2}}{\alpha^2_{H^{+}}}\right] = 0\text{V} - \frac{8.314\times 298.15}{2\times 96485}\ln\left[\frac{1}{(10^{-5.4})^2}\right]\text{V} = \text{-}0.319\text{V}$$

$$E^{\theta}_{H^{+}/H_2} = 0\text{V vs. SHE}$$

The overall reaction of discharging process along Zn oxidation and HER

$$Zn + 2H^{+} + 2OH^{-} \rightarrow ZnO + H_2 + H_2O$$

$$E_{theo}^{'} = E_c^{'} - E_a = -0.319\text{V} - (-1.219\text{V}) = 0.9\text{V}$$

During Charging, the following reactions are taking place at respective electrode:

At the cathode: (0.8 M $KHCO_3$, sat. CO_2 solution, (pH= 5.4):

$$H_2O \rightarrow \frac{1}{2}O_2 + 2H^{+} + 2e^{-}.$$

$$E_c^{''} = E_{H_2O/O_2}^{\theta} - \frac{RT}{nF}\ln\left[\frac{\alpha_{H_2O}}{\alpha_{O_2}^{1/2}\alpha_{H^+}^{2}}\right] = 1.229\text{V} - \frac{8.314\times 298.15}{2\times 96485}\ln\left[\frac{1}{1\times(10^{-5.4})^{2}}\right]V = 0.909\text{V}$$

$E_{H_2O/O_2}^{\theta} = 1.229\text{V}$ vs. SHE

At anode (6M KOH + 0.2M $(CH_3COO)_2$):

$$ZnO + H_2O + 2e^{-} \rightarrow Zn + 2OH^{-}$$

The overall reaction during charging is as follows:

$$ZnO + 2H_2O + 2e^{-} \rightarrow Zn + 2OH^{-}$$

$$E_{theo}^{''} = E_c^{''} - E_a = 0.909\text{V} - (-1.219\text{V}) = 2.128\text{V}$$

In the above theoretical potential calculations, the 0.8 M $KHCO_3$ solution (pH = 5.4) was considered. The CO_2 pre-saturation strategy was designed for the flow-type AZCB testing, that CO_2 gas was injected continuously in the $KHCO_3$ solution for 3 hrs. As CO_2 is dissolved in the $KHCO_3$ electrolyte, the followed chemical reaction occurs which results in the formation of K_2CO_3, H_2CO_3 and H_2O.

$$2KHCO_3 + CO_2 \rightarrow K_2CO_3 + \mathrm{H}_2CO_3 + H_2O$$

The produced H_2CO_3 is a weak acid which further dissociate into hydrogen ions (H^+) and bicarbonate ions HCO_3^- following the below reaction, therefore decreasing the electrolyte pH value to about 5.4 eventually.

$$H_2CO_3 \rightarrow HCO_3^- + H^+$$

So, the injection of CO_2 into KHCO3 medium makes the electrolyte solution becomes more and more acidic until the pH value to be about 5.4. For comparison, the Zn-BDC catalyst is also testified in the flow-type three-chamber AZCB using the same electrolytes, pre-saturation strategy, scan rates of the charge-discharge curve, CO_2 gas flow rate of 20 sccm, *etc*.

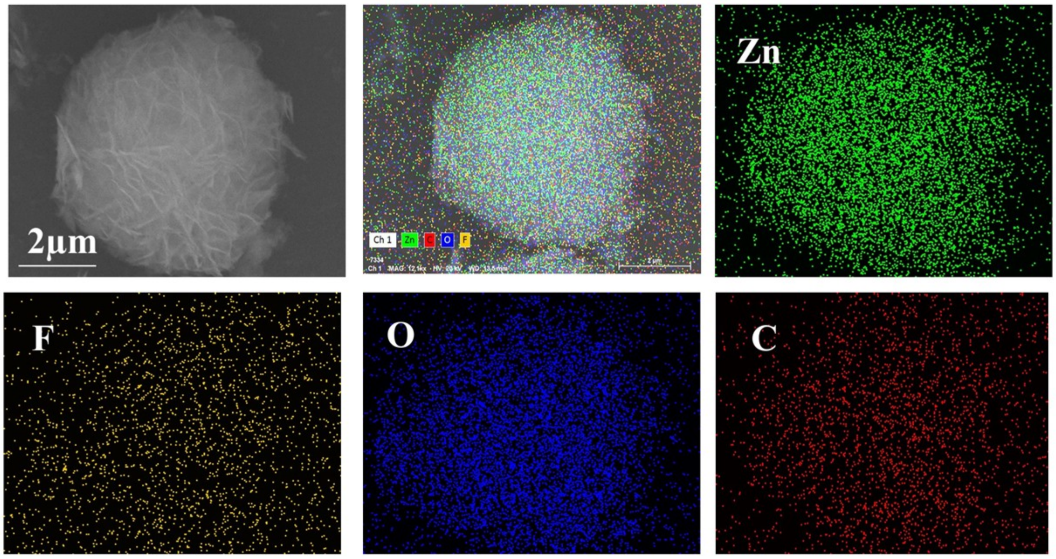

Figure S1. SEM images and EDX mapping of Zn, F, O and C of Zn-TFBDC.

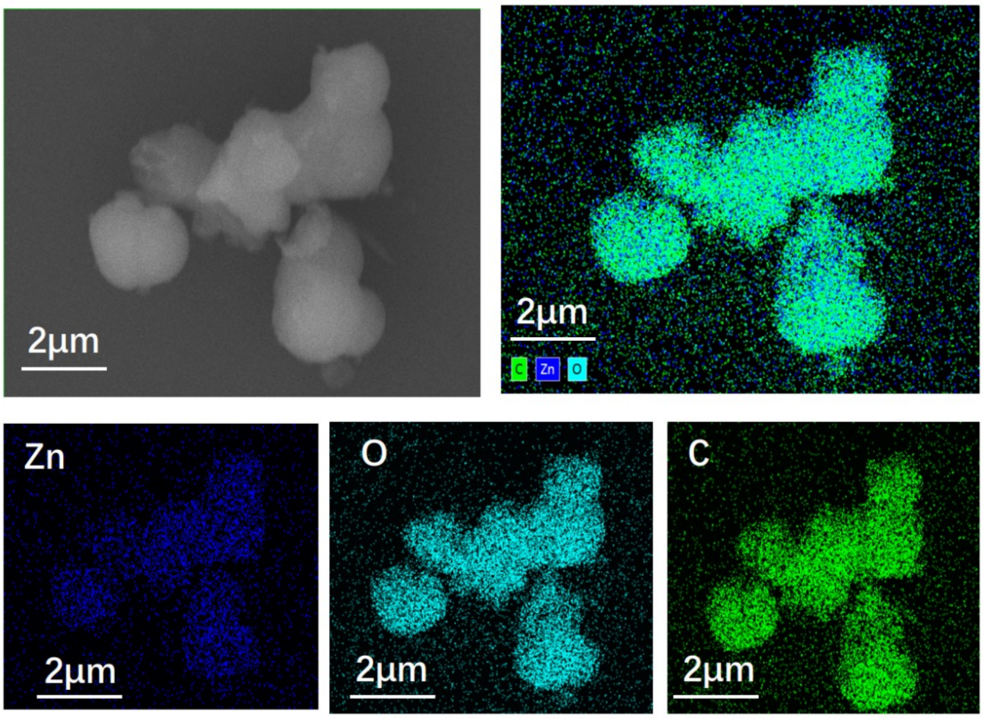

Figure S2. SEM image and its EDS mapping of Zn, O and C of Zn-BDC.

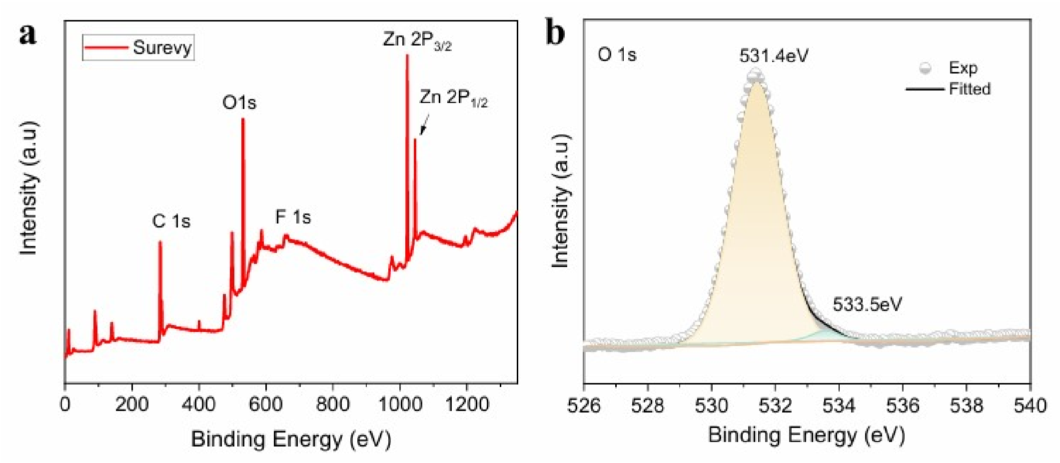

Figure S3. High resolution XPS spectra of Zn-TFBDC. (a) XPS survey spectrum; (b) O 1s spectrum.

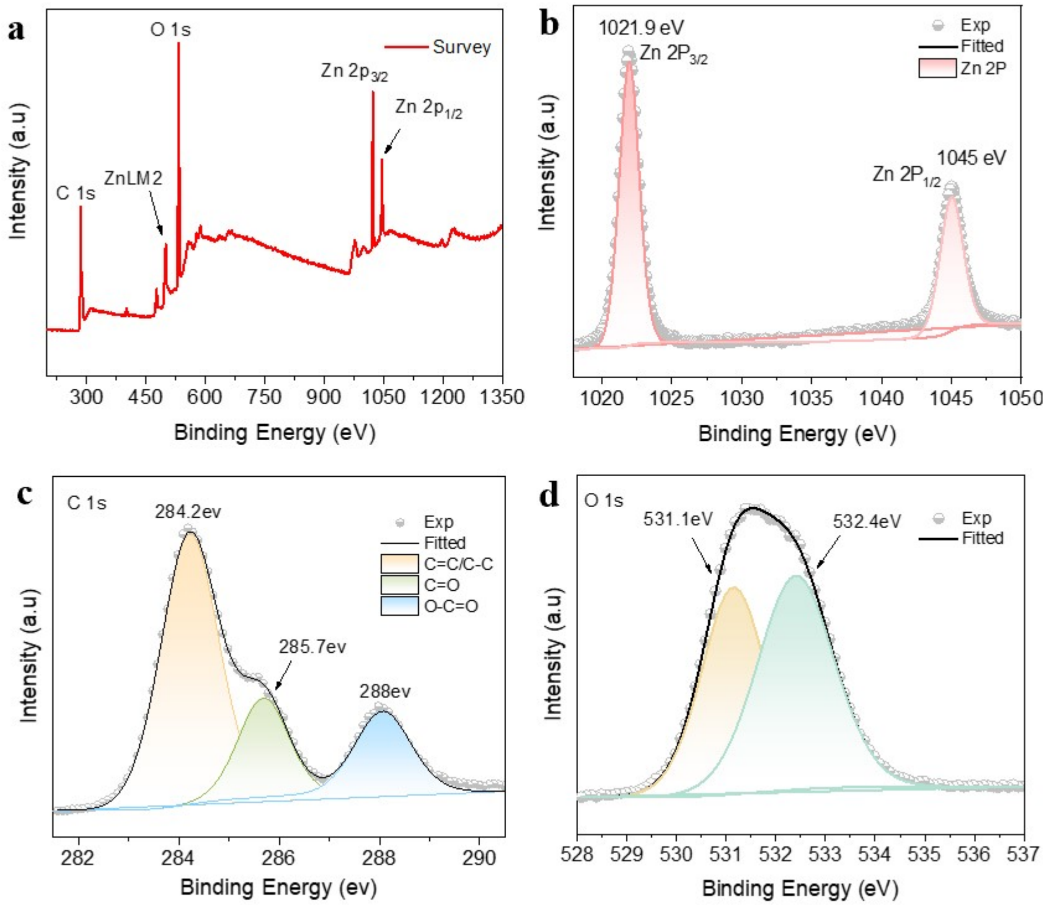

Figure S4. High resolution XPS spectra of Zn-BDC. (a) XPS survey spectrum; (b) Zn 2p; (c) C 1s; and (d) O 1s spectrum.

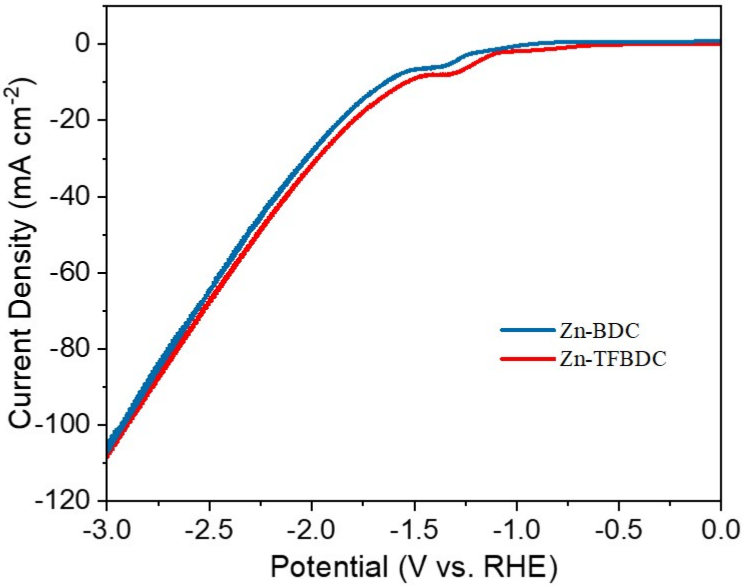

Figure S5. LSV curves of eCO$_2$RR using the Zn-TFBDC and Zn-BDC catalysts under CO$_2$ supply.

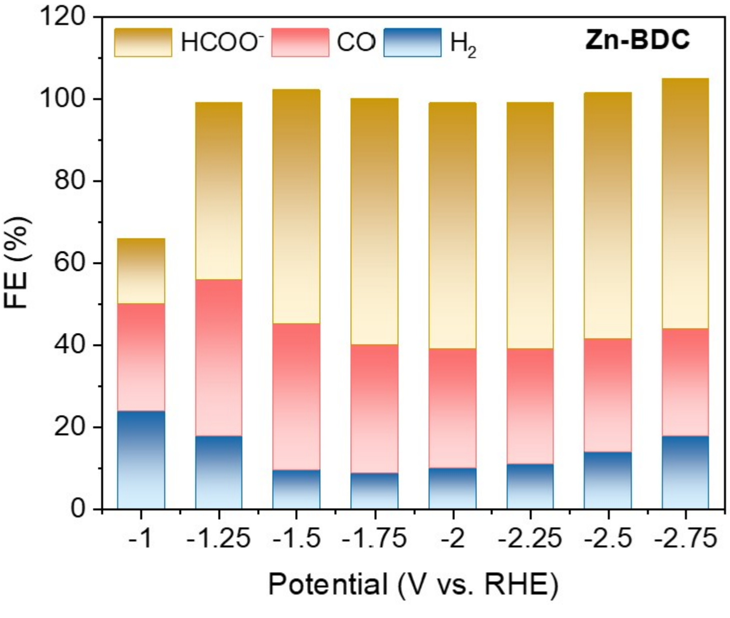

Figure S6. FE% of Zn-BDC promoted eCO$_2$RR at a potential window of -1 to -2.75 V vs RHE.

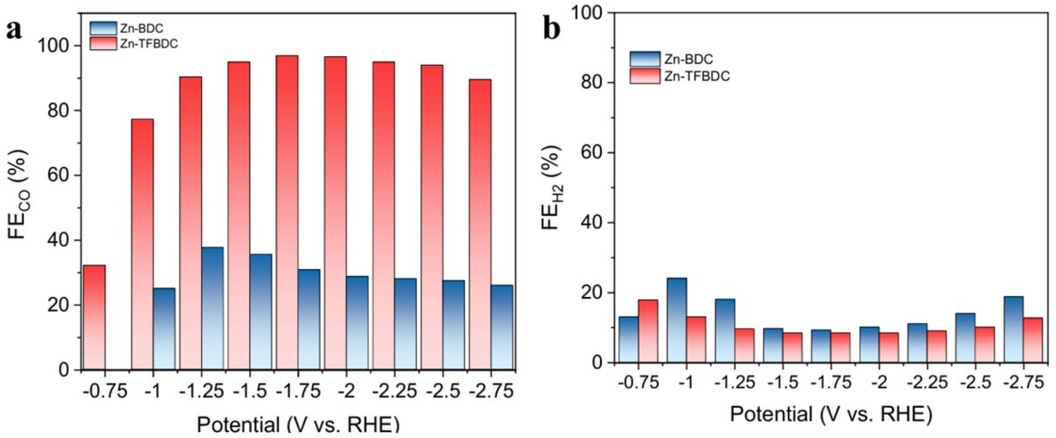

Figure S7. (a) The FE$_{CO}$ and (b) FE$_{H2}$ of eCO$_2$RR catalyzed by Zn-BDC and Zn-TFBDC.

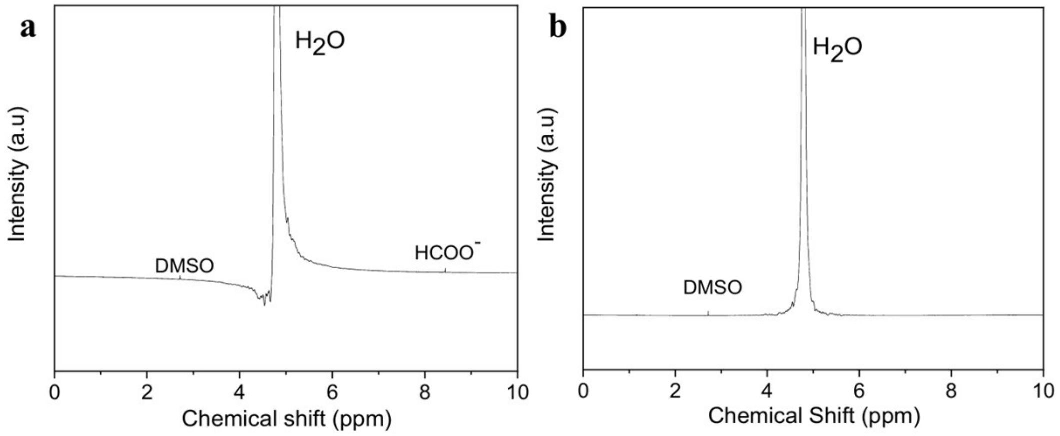

Figure S8. NMR spectra of eCO$_2$RR products using (a) Zn BDC, and (b) Zn-TFBDC catalysts under CO$_2$ supply.

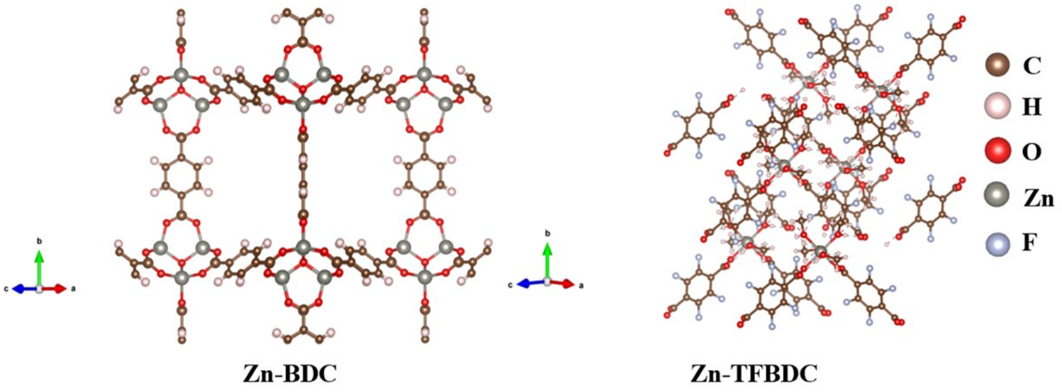

Figure S9. Modelling configurations for (a) Zn-BDC and (b) Zn-TFBDC.

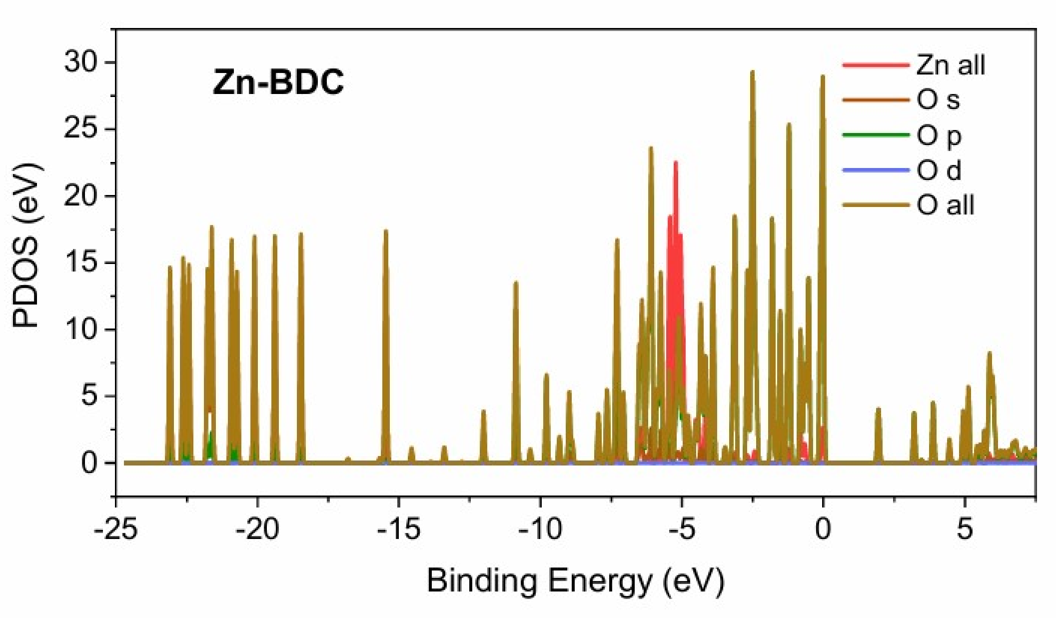

Figure S10. The density of state profile for Zn-BDC.

Figure S11. The pH value measured at different time during CO_2 dissolution.

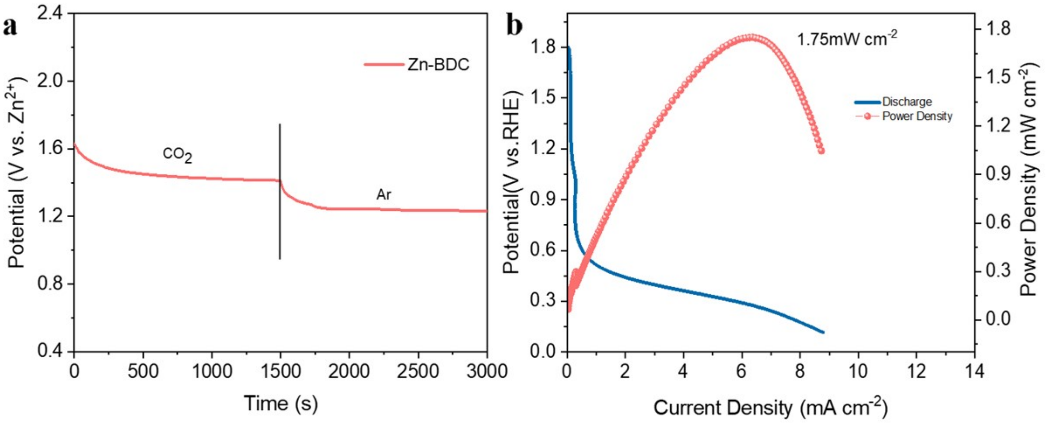

Figure S12. (a) OCP curves of the Zn-BDC constructed AZCB against CO_2 and Ar gases; (b) Discharge response along power density.

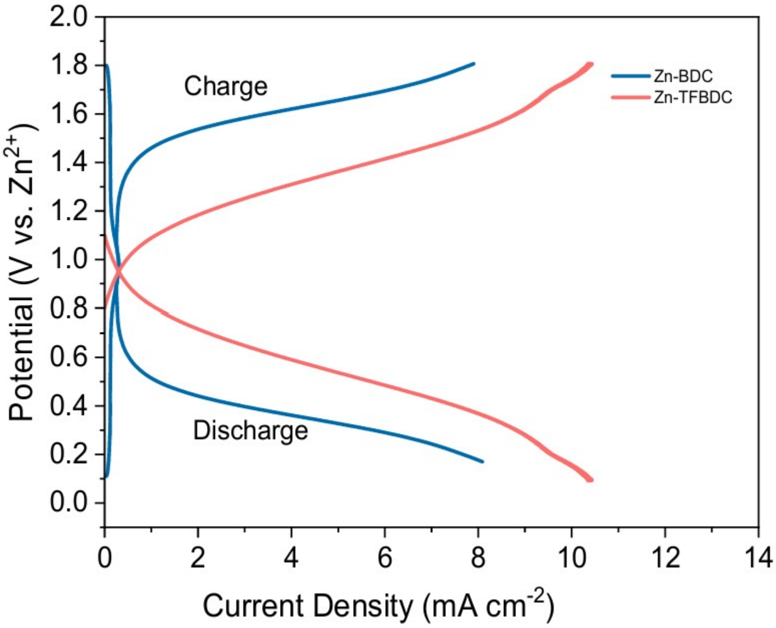

Figure S13. Polarization charge and discharge curves for AZCBs using Zn-BDC and Zn-TFBDC.

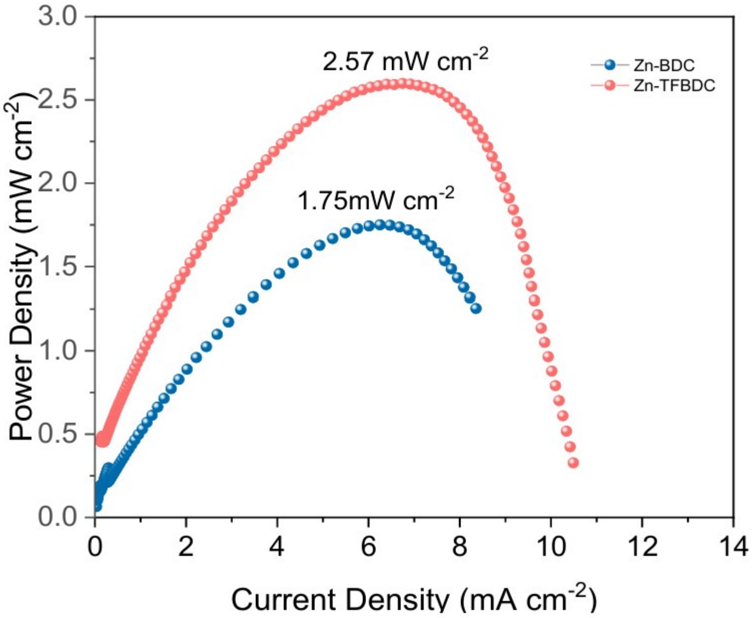

Figure S14. Power density curves for AZCBs using Zn-BDC and Zn-TFBDC.

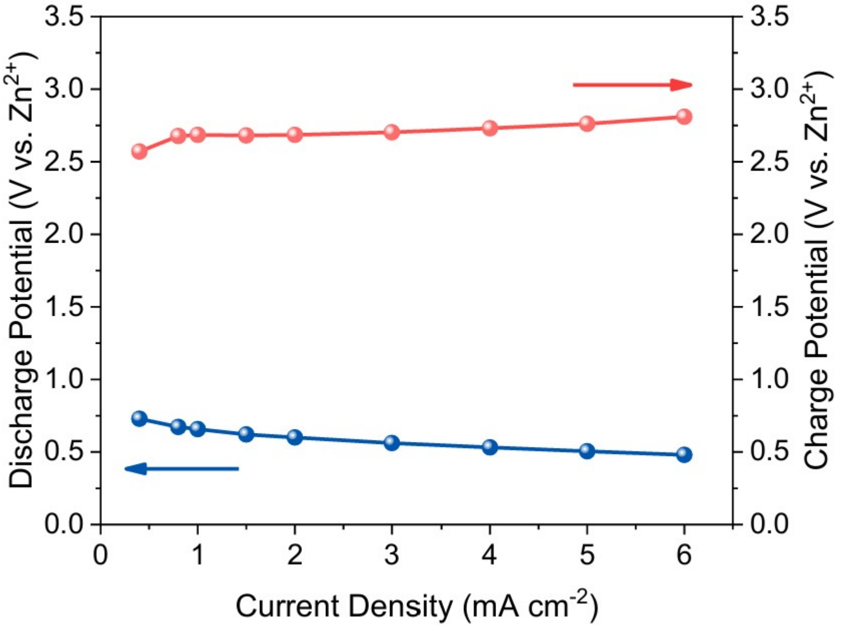

Figure S15. Overall charge and discharge response at different current densities for the AZCB using Zn-TFBDC.

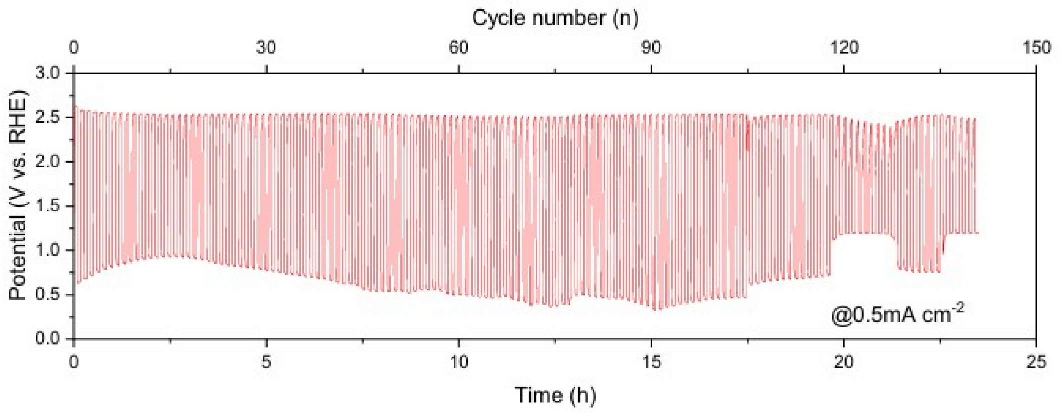

Figure S16. The Galvanostatic discharge-charge cyclability curve at a current density of 0.5 mA cm^{-2} for Zn-BDC constructed AZCB.

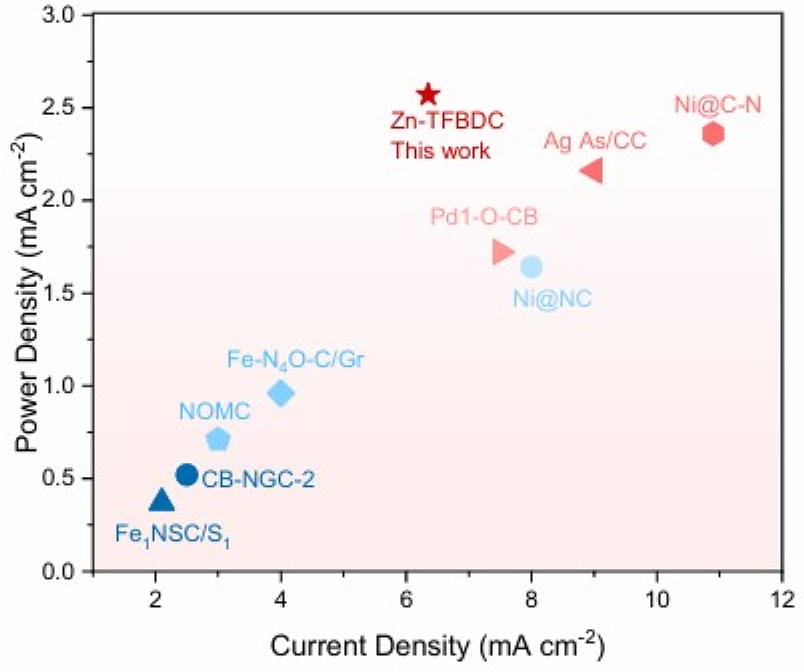

Figure S17. Comparison of power densities between this work and reported data with CO as the eCO$_2$RR product.

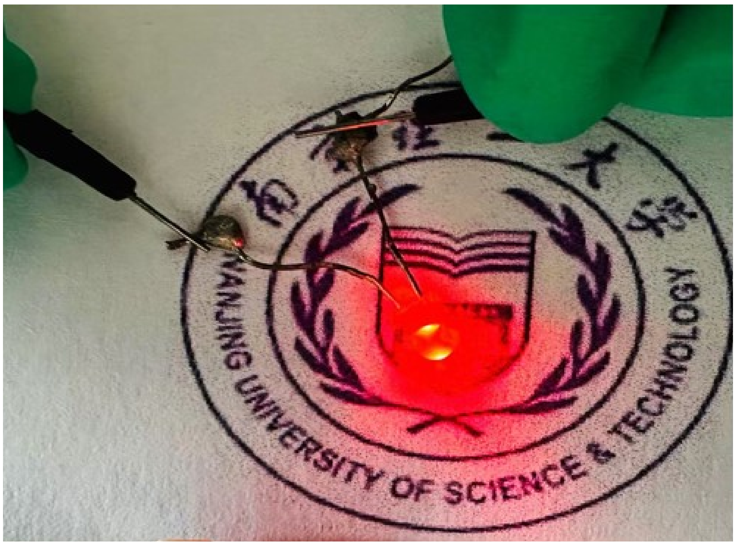

Figure S18. Digital photograph for single bulb illuminated by three series of An-TFBDC AZCBs.

Table S1. Comparison of FE_{HCOO^-} of eCO_2RR using as-prepared catalysts.

Potential (V vs.RHE)	Zn-BDC ($HCOO^-$) FE%	Zn-TFBDC ($HCOO^-$) FE%
-1	16	-
-1.25	43	-
-1.50	57	-
-1.75	60	-
-2.0	60	-
-2.25	60	-
-2.50	60	-
-2.75	61	-

Table S2. Reported performance summary of AZCBs.

Electrocatalyst	**Cell type**	**Electrolyte**	**OCP (V)**	**Discharge voltage (V)**	**Power density ($mW\ cm^{-2}$)**	**Reference**
Zn-TFBDC	**Flow Cell**	**Catholyte:** **0.8 M $KHCO_3$** **Anolyte:** **6 M KOH + 0.2 M $Zn(ac)_2$**	**1.5**	**0.404**	**2.57 (6.35 mA cm^{-2})**	**This Work**
Fe_1NC/S_1-1000 (Dispersed Fe in N doped porous carbon)	Flow Cell	**Catholyte:** 0.8 M $KHCO_3$ **Anolyte:** 0.8 M KOH + 0.02 M $Zn(ac)_2$	0.72	0.21	0.52 (2.5 mA cm^{-2})	*J. Adv. Mater.*, 2020, 32, 2002430
P-Ag/CP (porous silver film)	H-Cell	**Catholyte:** 0.8 M $KHCO_3$ **Anolyte:** 6 M KOH + 0.2 M $Zn(ac)_2$	0.9	0.18	0.37 (2.1 mA cm^{-2})	*Nanoscale*, 2024, 16, 10628-10636
Ni@NC (N-doped carbon shell)	Flow Cell	**Catholyte:** 1 M $KHCO_3$ **Anolyte:** 6 M KOH + 0.2 M $Zn(ac)_2$	-	0.2	1.64 (8 mA cm^{-2})	*Small*, 2023, 19, 2301128

Fe-N$_4$O-C/ Gr nanoplates	Flow Cell	**Catholyte:** 0.5 M $KHCO_3$ **Anolyte:** 6 M KOH + 0.2 M $Zn(ac)_2$	0.7	0.25	0.96 (4 mA cm^{-2})	*Adv. Funct. Mater.*, 2023, 33, 2300801
Ag As /CC (Ag aerogel conductive carbon cloth)	Flow Cell	**Catholyte:** 1 M $KHCO_3$ **Anolyte:** 6 M KOH + 0.02 M $Zn(ac)_2$	-	0.24	2.16 (9.0 mA cm^{-2})	*Chem. Eng. Sci.*, 2023, 280, 119042
Coralloid Au	H-Cell	**Catholyte:** 0.5 M $KHCO_3$ **Anolyte:** 6 M KOH + 0.2 M $Zn(acc)_2$	-	0.34	0.7 (2.4 mA cm^{-2})	*J. Mater. Chem. A.*, 2021, 9, 21024-21031
Pd1-O-CB	Flow Cell	**Catholyte:** 0.5 M $KHCO_3$ **Anolyte:** 6 M KOH + 0.02 M $Zn(ac)_2$	0.8	0.22	1.72 (7.8 mA cm^{-2})	*J. Chem. Eng.*, 2023, 461, 141865
Fe-P@NCPs	H-Cell	**Catholyte:** 1 M $KHCO_3$ **Anolyte:** 6 M KOH + 0.02 M $Zn(ac)_2$	0.69	0.3	0.86 (3.2 mA cm^{-2})	*Small*, 2022, 18, 2104965
FeNC NSs-1000	Flow Cell	**Catholyte:** 0.5 M $KHCO_3$ **Anolyte:** 6 M KOH + 0.2 M $Zn(ac)_2$	-	0.58	1.05 (1.8 mA cm^{-2})	*Nano Energy*, 2023, 113, 108568
$La_2Cu_{0.95}P_{0.05}O_4$	Flow Cell	**Catholyte:** 1 M $KHCO_3$ **Anolyte:** 0.5 M KOH + 0.2 M $Zn(ac)_2$	-	0.38	0.75 (2.2 mA cm^{-2})	*Energy*, 2023, 263, 125688
Fe@NPC	Flow Cell	**Catholyte:** 1 M $KHCO_3$ **Anolyte:** 6 M KOH + 0.2 M $Zn(ac)_2$	-	0.25	3 (13 mA cm^{-2})	*J. Catal.*, 2023, 48, 185-194

Ni@C-N	Flow Cell	**Catholyte:** 1 M $KHCO_3$ **Anolyte:** 6 M KOH	0.78	0.22	2.36 (10.9 mA cm^{-2})	*J. Mater. Chem. A.*, 2024, 12, 9462-9468
H-Ni9Cu1@NCNTs/CFM	Flow Cell	**Catholyte:** 0.5 M $KHCO_3$ **Anolyte:** 6 M KOH + 0.2 M $Zn(ac)_2$	-	0.35	0.62 (2.25 mA cm^{-2})	*Chin. Chem. Lett.*, 2022, 33, 3721-3725
CoPc/S-NHC	H-Cell	**Catholyte:** 0.5 M $KHCO_3$ **Anolyte:** 6 M KOH + 0.2 M $Zn(ac)_2$	1.57	0.6	2.68 (4.7 mA cm^{-2})	*Adv. Funct. Mater.*, 2024, 34, 2312552
CB-NGC-2 (Ceder biomass N-doped graphitized carbon)	Flow Cell	**Catholyte:** 0.8 M $KHCO_3$ **Anolyte:** 0.8 M KOH + 0.2 M $Zn(ac)_2$	0.79	0.25	0.51 (2.14 mA cm^{-2})	*ACS Appl. Mater. Interfaces*, 2021, 13, 3738-3747
NOMC (N-doped ordered mesoporous Carbon)	H-Cell	**Catholyte:** 0.8 M $KHCO_3$ **Anolyte:** 6 M KOH + 0.2 M $Zn(ac)_2$	0.9	0.25	0.71 (3 mA cm^{-2})	*Small Methods*, 2021, 5, 2001039

References

1. J. Hutter, M. Iannuzzi, F. Schiffmann and J. VandeVondele, *Wiley Interdiscip. Rev. Comput. Mol. Sci.*, 2014, **4**, 15-25.
2. J. VandeVondele and J. Hutter, *J. Chem. Phys.*, 2007, **127**, 114105.
3. M. Krack, *Theor. Chem. Acc.*, 2005, **114**, 145-152.
4. T. Lu and F. Chen, *J. Comput. Chem.*, 2012, **33**, 580-592.
5. T. Lu and Q. Chen, *J. Comput. Theor. Chem.*, 2021, **1200**, 113249.